TABLE I. Screening radius as a function of valence difference for impurities in silver.

Z	−3	−2	−1	+1	+2	+3	+4
r_s (A)	0.73	0.7	0.665	0.5	0.485	0.473	0.468

equal the valence difference (Friedel sum rule), one then finds the r_s is, for a given solvent metal, also a function of Z.

The correct screening radii for fulfilling the Friedel condition have been evaluated for impurities in silver. The results are listed in Table I. The form of the potential, namely (Z/r) exp$(-r/r_s)$, was assumed a priori, and r_s was treated as an adjustable parameter. In Fig. 1 are shown the activation energies for solute diffusion calculated from these screening radii using the formula derived by Lazarus, as well as the experimental activation energies and those obtained by using the screening radius predicted by the Fermi-Thomas model.

There may be a number of reasons for the discrepancy between the calculated and experimental results. The theory proposed by Lazarus is admittedly only semi-quantitative. Also, the assumption of a screened Coulomb potential neglects all effects due to the size of the ion core, although this may play a significant role.

In any case, a significant feature of the results is the marked asymmetry of the calculated activation energies about the point $Z=0$. This asymmetry is a consequence of the dependence of r_s on Z, shown in Table I, which gives rise to much larger screening radii for negative than for positive Z values. One may, therefore, predict from this dependence of r_s on Z that the absolute magnitude of the difference in activation energies for solute
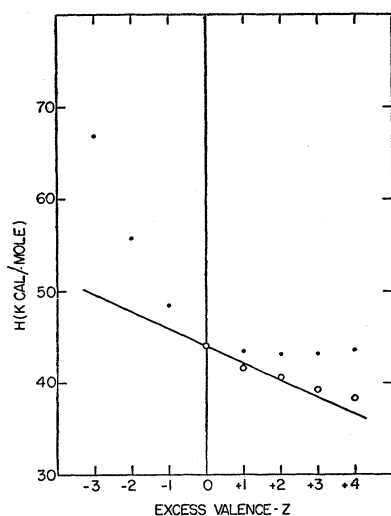

FIG. 1. Calculated and experimental activation energies for solute diffusion in silver. The straight line results from the use of a constant screening radius given by the Fermi-Thomas model. The solid points were calculated with the screening radii listed in Table I. The circles show the experimental results.

and self-diffusion should be significantly larger for solutes which are electropositive relative to the solvent than for the corresponding electronegative solutes. This conclusion appears to be confirmed by preliminary measurements on the diffusion of ruthenium in silver.[6]

The author is grateful to Professor D. Lazarus, Professor L. Slifkin, and Dr. C. T. Tomizuka for several stimulating conversations, and to Dr. S. Machlup for his generous help in preparing the numerical work for machine computation by the ILLIAC.

Energy Distribution of Neutrons Scattered by Paramagnetic Substances

B. N. BROCKHOUSE

Physics Division, Atomic Energy of Canada Limited, Chalk River, Ontario, Canada

SLOW neutrons, when scattered magnetically by a paramagnetic material, undergo an energy change which depends on the degree of coupling of the magnetic ions. Van Vleck[1] has calculated the energy changes expected for paramagnetic substances in which the coupling arises from exchange forces. In a high-temperature approximation he finds that the rms energy change

$$(\delta E)_{\rm rms} = k_B |\Delta| [6/ZS(S+1)]^{\frac{1}{2}}, \qquad (1)$$

where k_B is Boltzmann's constant, Z is the number of interacting neighbors, S is the spin of the ion and Δ is the Weiss constant determined from the measured susceptibility by fitting to the Curie Weiss law $\chi = C/(T-\Delta)$. Van Vleck was not able to obtain a detailed energy distribution but a calculation of the fourth moment suggested that a Gaussian might be a fair approximation.

By using the apparatus shown in Fig. 1, the energy distribution of neutrons scattered by a number of paramagnetic substances has been measured. Neutrons of wavelength λ_0 in the region of 1.3 angstroms (energy 0.05 ev) are selected from the NRX reactor spectrum by a crystal (X1). A small fraction (usually about 10 percent) of the resulting monoenergetic neutrons is scattered by the specimen, and the energy distribution of those scattered at some particular angle ϕ is examined by means of an analzying crystal spectrometer (X2). Background is obtained by turning the crystal (X2) by an amount such that the Bragg law can no longer be satisfied for any neutron energy. This is done automatically at intervals during a run. A background so
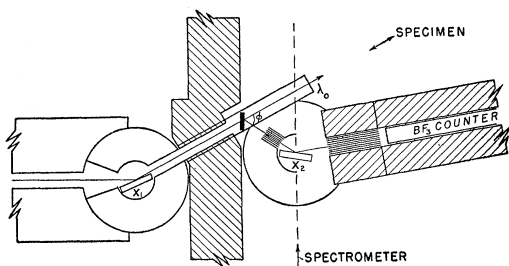
FIG. 1. Schematic diagram of the apparatus. The angle of scattering ϕ can be changed by moving the specimen and the spectrometer as indicated.

determined has been subtracted in the results following. The energy distributions are normalized to the counting rate obtained with the counter looking directly at the specimen and can be put on an absolute basis by comparison with similar measurements on a vanadium standard. The scattering by vanadium metal, which is almost completely incoherent, consists,[2,3] of a widely spreading inelastic component which increases with angle of scattering and temperature, and a truly elastic component which falls off with angle of scattering and temperature according to a Debye-Waller factor. The shape of this elastic peak is taken to represent the resolution function of the instrument at the incident energy. A rough intensity calibration has been obtained by theoretical considerations[4] and by
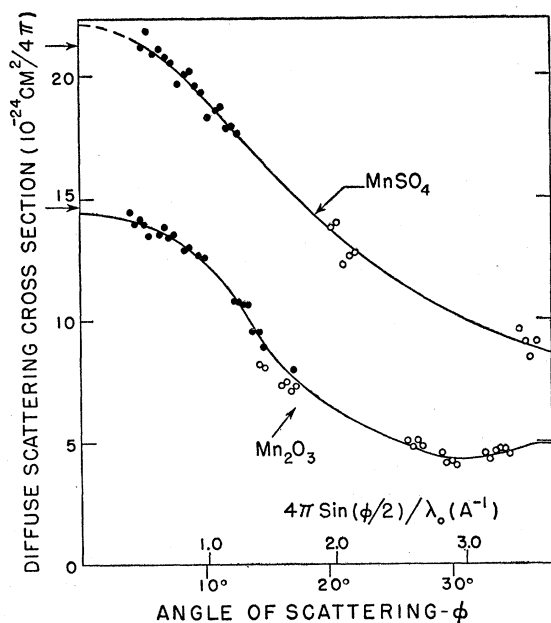

FIG. 2. Differential cross section (barns/4π steradians) of MnSO$_4$ and Mn$_2$O$_3$ for 1.12 A neutrons at 295°K. The observed scattering is composed of magnetic and thermal diffuse scattering, the latter being almost zero at zero angle of scattering. Multiple and incoherent scattering has been subtracted. The horizontal arrows indicate the theoretical magnetic cross sections at zero scattering angle for 5 spins and 4 spins. Different symbols indicate the results of different experiments.

measuring the energy distribution of neutrons scattered by a thick ($\sim$10 mean free paths) paraffin scatterer and assuming them to be Maxwellian.

Measurements were made on anhydrous specimens of MnSO$_4$ and Mn$_2$O$_3$.

MnSO$_4$.—In this substance the coupling between the manganese ions is small as indicated by the Weiss constant[5] of $\Delta = -24°$ and the fact that the transition temperature is less than 14°K. The angular distribution of the scattered neutrons,[6] Fig. 2, shows no structure which might be attributable to effects of coupling.

The energy distribution of neutrons scattered with the momentum change $4\pi \sin(\phi/2)/\lambda_0 = 0.97$ A^{-1} is shown in Fig. 3(a). The points were fitted to the resolu-
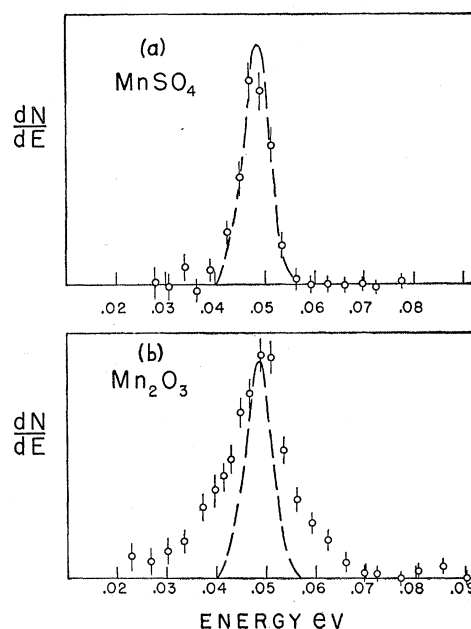

FIG. 3. Energy distributions of neutrons of wavelength 1.28$_8$ A after scattering by MnSO$_4$ and Mn$_2$O$_3$ at an angle of 11°20'. Within the accuracy the spectra contain all the scattered neutrons. A component of each spectrum is multiply scattered amounting to 11 percent in the case of MnSO$_4$ and 9 percent in the case of Mn$_2$O$_3$. The resolution function for the instrument is shown as dashed lines. In the case of MnSO$_4$ it was fitted to the points by area normalization.

tion function for the instrument by area normalization. Within the accuracy, no perceptible energy changes occur, in agreement with Eq. (1).

Mn$_2$O$_3$.—In this substance the coupling between manganese ions is appreciable since the transition temperature[7] is 80°K and the Weiss constant[8] $\Delta = -176°$. The angular distribution, Fig. 2, possibly shows some structure.

The energy distribution is shown in Fig. 3(b). The distribution is asymmetrical by about the amount of a Boltzmann factor, $\exp(-\delta E/k_B T)$. The half-width of the distribution is somewhat greater than that given by Eq. (1) (0.0043 ev or 51°K), but by no more than might

be expected from the uncertainties in both the theory and the experiment.

Work has been done on a number of other materials including MnO, Cr_2O_3, and $ZnFe_2O_4$ and is being continued with a view to studying the dependence of the energy distribution on the temperature, the angle of scattering, and the degree of magnetic order. An account of this work will be submitted to the *Canadian Journal of Physics*.

The author is indebted to Dr. D. G. Henshaw for the excellent aluminum crystals used in these experiments.

[1] J. H. Van Vleck, Phys. Rev. **55**, 924 (1939).
[2] J. M. Cassels, *Progress in Nuclear Physics* (Academic Press, Inc., New York, 1950), Vol. 1.
[3] Energy distributions of neutrons scattered by vanadium metal under several different conditions have been measured by the author with results in agreement with the theory. This work is being continued with a view to obtaining the frequency distribution of the normal modes in vanadium metal.
[4] G. E. Bacon and R. D. Lowde, Acta Cryst. **1**, 303 (1948).
[5] de Haas, Schultz, and Koolhass, Chem. Abstracts **34**, 2222² (1940); Physica **7**, 57 (1940).
[6] See also Shull, Strauser, and Wollan, Phys. Rev. **83**, 333 (1951).
[7] E. G. King, J. Am. Chem. Soc. **76**, 3289 (1954).
[8] Bhatnagar, Cameron, Harbard, Kapur, King, and Prakash, J. Chem. Soc. 1433 (1939).

Annealing Process in Neutron-Irradiated LiF

D. BINDER AND W. J. STURM

Oak Ridge National Laboratory, Oak Ridge, Tennessee

(Received May 12, 1955)

THE previous work[1] on neutron irradiated LiF crystals showed that the lattice expansion was caused by equal numbers of vacancies and interstitial atoms. It was also shown, by analyzing the annealing data for nonuniformly irradiated crystals, that the annealing process was of order higher than one. We will now derive a more exact order, an activation energy, and a jump frequency for the lattice defects causing the expansion by analyzing the annealing data for uniformly irradiated crystals.

As described previously,[1] two crystals were covered with 0.03 in. of cadmium during irradiation to insure a uniform irradiation. The lattice parameter changes as derived from density measurements, $(\Delta a/a)_\rho$, for the crystals after irradiation and after 10-minute anneals

TABLE I. The lattice parameter changes after irradiation and successive thermal anneals.

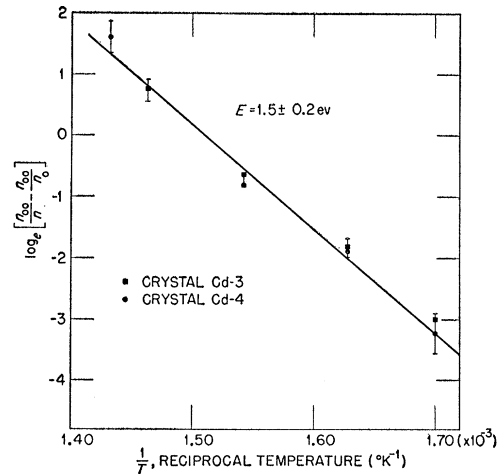| Condition	$10^4(\Delta a/a)_\rho$ Crystal Cd-3	Crystal Cd-4
Irradiated	8.02	8.51
315°C anneal	7.65	8.16
345	6.64	7.08
375	4.62	5.18
410	2.06	...
425	...	1.25

FIG. 1. Annealing data assuming a second-order process.

at successively higher temperatures, are summarized in Table I. The probable error in $(\Delta a/a)_\rho$ is $\pm 1.3 \times 10^{-5}$, and the blank spaces represent anneals not performed.

Assume that the lattice defects change position by a random walk process. Then if we have a single rate process with activation energy E for unit motion, the probability for taking one step at temperature T varies as $e^{-E/kT}$, and the rate of change of the total defect concentration n is

$$dn/dt = -cn^\gamma e^{-E/kT},$$

where c is a constant and γ is the order of the reaction. The solution of this equation for $\gamma > 1$ may be expressed in the form,

$$\log_e\{(n_{00}/n)^{\gamma-1} - (n_{00}/n_0)^{\gamma-1}\} = \log_e\{(\gamma-1)n_{00}^{\gamma-1}ct\} - E/kT, \quad (1)$$

where n_{00} is the defect concentration for the irradiated condition and n_0 is the concentration for the start of each anneal at temperature T.

We assume n is proportional to $(\Delta a/a)_\rho$ so that both n_{00}/n and n_{00}/n_0 may be determined from ratios of the data in Table I. Since the anneals were performed for a fixed time interval, the plot of $\log_e\{(n_{00}/n)^{\gamma-1} - (n_{00}/n_0)^{\gamma-1}\}$ *versus* $1/T$ should be a straight line for the correct order γ, and the slope should determine the activation energy. A straight line is obtained for $\gamma = 2$, as shown in Fig. 1, and the slope indicates an activation energy of 1.5 ± 0.1 ev. The possibility of $\gamma = 1$ was eliminated in reference 1, and the plot for $\gamma = 3$ is curved as shown in Fig. 2. The annealing process is then of the second order as expected from the random recombination of non-neighboring, isolated vacancies and interstitials, or Frenkel defects.

Keating[2] has suggested that the irradiation-induced distortion cannot be due to isolated vacancies and interstitials, but to large aggregates of imperfections. His data show a lattice expansion only one-tenth as